A Large-Scale Model of the Functioning Brain

Chris Eliasmith,* Terrence C. Stewart, Xuan Choo, Trevor Bekolay, Travis DeWolf, Charlie Tang, Daniel Rasmussen

A central challenge for cognitive and systems neuroscience is to relate the incredibly complex behavior of animals to the equally complex activity of their brains. Recently described, large-scale neural models have not bridged this gap between neural activity and biological function. In this work, we present a 2.5-million-neuron model of the brain (called "Spaun") that bridges this gap by exhibiting many different behaviors. The model is presented only with visual image sequences, and it draws all of its responses with a physically modeled arm. Although simplified, the model captures many aspects of neuroanatomy, neurophysiology, and psychological behavior, which we demonstrate via eight diverse tasks.

Large-scale neural simulations are becoming increasingly common [see (*1*) for a review]. These include the ambitious Blue Brain Project (*2*), which has simulated about 1 million neurons in cortical columns and includes considerable biological detail, accurately reflecting spatial structure, connectivity statistics, and other neural properties. More recent work has simulated many more neurons, such as the 1 billion neurons simulated in the Cognitive Computation Project (*3*), which has been hailed as a cat-scale simulation. A human-scale simulation of 100 billion neurons has also been reported (*4*).

Although impressive scaling has been achieved, no previous large-scale spiking neuron models have demonstrated how such simulations connect to a variety of specific observable behaviors. The focus of this past work has been on scaling to larger numbers of neurons and more detailed neuron models. Unfortunately, simulating a complex brain alone does not address one of the central challenges for neuroscience: explaining how complex brain activity generates complex behavior. In contrast, we present here a spiking neuron model of 2.5 million neurons that is centrally directed to bridging the brain-behavior gap. Our model embodies neuroanatomical and neurophysiological constraints, making it directly comparable to neural data at many levels of analysis. Critically, the model can perform a wide variety of behaviorally relevant functions. We show results on eight different tasks that are performed by the same model, without modification.

All inputs to the model are 28 by 28 images of handwritten or typed characters. All outputs are the movements of a physically modeled arm that has mass, length, inertia, etc. For convenience, we refer to the model as "Spaun" (Semantic Pointer Architecture Unified Network) (see Fig. 1 and supplementary materials and methods section S1.1). Many of the tasks we have chosen are the subject of extensive modeling in their own right [e.g., image recognition (*5*, *6*), serial working memory (WM) (*7*, *8*), and reinforcement learning (RL) (*9*, *10*)], and others demonstrate abilities that are rare for neural network research and have not yet been demonstrated in spiking networks (e.g., counting, question answering, rapid variable creation, and fluid reasoning). The eight tasks (termed "A0" to "A7") that Spaun performs are: (A0) Copy drawing. Given a randomly chosen handwritten digit, Spaun should produce the same digit written in the same style as the handwriting (movie S1; all supplemental movies can be viewed at http://nengo.ca/build-a-brain/spaunvideos). (A1) Image recognition. Given a randomly chosen handwritten digit, Spaun should produce the same digit written in its default writing (movie S2). (A2) RL. Spaun should perform a three-armed bandit task, in which it must determine which of three possible choices generates the greatest stochastically generated reward. Reward contingencies can change from trial to trial (movie S3). (A3) Serial WM. Given a list of any length, Spaun should reproduce it (movie S4). (A4) Counting. Given a starting value and a count value, Spaun should write the final value (that is, the sum of the two values) (movie S5). (A5) Question answering. Given a list of numbers, Spaun should answer either one of two possible questions: (i) what is in a given position in the list? (a "P" question) or (ii) given a kind of number, at what position is this number in the list? (a "K" question) (movie S6). (A6) Rapid variable creation. Given example syntactic input/output patterns (e.g., 0 0 7 4 → 7 4; 0 0 2 4 → 2 4; etc.), Spaun should complete a novel pattern given only the input (e.g., 0 0 1 4 → ?) (movie S7). (A7) Fluid reasoning. Spaun should perform a syntactic or semantic reasoning task that is isomorphic to the induction problems from the Raven's Progressive Matrices (RPM) test for fluid intelligence (*11*). This task requires completing patterns of the form: 1 2 3; 5 6 7; 3 4 ? (movie S8). Each input image is shown for 150 ms and separated by a 150-ms blank (see table S2 for example inputs for each task). The model is told what the task will be by showing it an "A" and the number of the task (0 to 7). The model is then shown input defining the task (see Figs. 2 and 3 for examples). Spaun is robust to invalid input (fig. S10) and performs tasks in any order without modeler intervention.

Figure 1A shows the anatomical architecture of the model. Connectivity and functional ascriptions to brain areas in Spaun are consistent with current empirical evidence (table S1). In general, we modeled neuron and synaptic response properties on the electrophysiology literature for the relevant anatomical areas. For instance, the basal ganglia have largely GABAergic neurons, with dopamine modulating learning in the striatum, and the cortex has largely *N*-methyl-D-aspartate and AMPA synaptic connections (supplementary section S1.3). As a result, the dynamics in the model are tightly constrained by underlying neural properties (see supplementary section S2.4).

The functional architecture of the model is described in Fig. 1B. The network implementing the Spaun model consists of three compression hierarchies, an action-selection mechanism, and five subsystems. Components of the model communicate using spiking neurons that implement neural representations that we call "semantic pointers," using various firing patterns. Semantic pointers can be understood as being elements of a compressed neural vector space (supplementary sections S1.1 and S1.2). Compression is a natural way to understand much of neural processing. For instance, the number of cells in the visual hierarchy gradually decreases from the primary visual cortex (V1) to the inferior temporal cortex (IT) (*12*), meaning that the information has been compressed from a higher-dimensional (image-based) space into a lower-dimensional (feature) space (supplementary section S1.3). This same kind of operation maps well to the motor hierarchy (*13*), where lower-dimensional firing patterns are successively decompressed (for example, when a lower-dimensional motor representation in Euclidean space moves down the motor hierarchy to higher-dimensional muscle space).

Compression is functionally important because low-dimensional representations can be more efficiently manipulated for a variety of neural computations. Consequently, learning or defining different compression/decompression operations provides a means of generating neural representations that are well suited to a variety of neural computations. The specific compression hierarchies in Spaun are (see Fig. 1B): (i) a visual hierarchy, which compresses image input into lower-dimensional firing patterns; (ii) a motor hierarchy that decompresses firing patterns in a low-dimensional space to drive a simulated arm; and (iii) a WM, which constructs compressed firing patterns to store serial position information. The WM subsystem includes several subcomponents that provide stable representations of intermediate task states, task subgoals, and context.

Spaun's action-selection mechanism is based on a spiking basal ganglia model that we have developed in other work (*14*) but is here extended to process higher-dimensional neural representations. The basal ganglia determine which state the network should be in, switching as appropriate for the current task goals. Consequently, the model's functional states are not hardwired, as the basal ganglia are able to control the order of operations by changing information flow between subsystems of the architecture.

The five subsystems, from left to right in Fig. 1B, are used to: (i) map the visual hierarchy firing pattern to a conceptual firing pattern as needed

Centre for Theoretical Neuroscience, University of Waterloo, Waterloo, ON N2J 3G1, Canada.

*To whom correspondence should be addressed. E-mail: celiasmith@uwaterloo.ca

(information encoding), (ii) extract relations between input elements (transformation calculation), (iii) evaluate the reward associated with the input (reward evaluation), (iv) decompress firing patterns from memory to conceptual firing pattern (information decoding), and (v) map conceptual firing patterns to motor firing patterns and control motor timing (motor processing). Supplementary materials section S1.3 includes a more detailed description of each element. It is critical to note that the elements of Spaun are not task-specific. That is, they are used in a variety of combinations to perform the chosen tasks, resulting in the same circuitry being used across tasks. This makes it straightforward to extend the model to some new tasks (supplementary section S2.4).

The neural connection weights of these subsystems can be learned with a biologically plausible spike-based rule (*15*), although we use more efficient optimization methods to determine the synaptic weights (supplementary section S1.2).

To help explain the functioning of the model, we consider the serial WM task. Figure 2A shows the information flow through the model for this task. The storage and recall states of the network are common to many tasks. For the WM task, these states occur immediately one after the other, although the delay is task-dependent. Initially, seeing the task identifier (A3) switches Spaun into the storage state. In the storage state, the network compresses the incoming image into a visually based firing pattern (FP in the figure) that encodes visual features, maps that firing pattern to another firing pattern that represents the related concept (e.g., "TWO"; see supplementary section S1.3), and then compresses that firing pattern into a memory trace that is stored in WM. The compression operator (i.e., "⊗") binds the concept firing pattern (e.g., TWO) to a position representation (e.g., P3) and adds the result (i.e., TWO ⊗ P3, as in Fig. 2C) to WM. As shown in Fig. 2C, this process is repeated as long as items are shown to the model.

Figure 2B shows a screen capture from a movie of the WM simulation. When the model sees the "?" input (as in Fig. 2B), the basal ganglia reroute cortical connectivity to allow Spaun to recall the input stored in the dorsolateral prefrontal cortex (DLPFC). Recall consists of decompressing an item from the stored representation of the full list, mapping the resulting concept vector to a known high-level motor command, and then decompressing that motor command to specific joint torques to move the arm. This process is repeated for each position in the WM, to generate Spaun's full written response. Figure 2C shows the entire process unfolding over time, including spike rasters, conceptual decodings of the contents of DLPFC, and the input and output.

Critically, no single task captures the distinct features of this model. To highlight the diversity of tasks the model is able to perform, Fig. 3 shows the results of the model performing a low-level perceptual-motor task (the copy-drawing task), as well as a challenging pattern-induction task only performed by humans (the RPM task).

Specifically, Fig. 3A demonstrates that the low-level perceptual features in the input are available to Spaun to drive its motor behavior. Figure 3B demonstrates the RPM task for one sample pattern (see fig. S6 for an additional example). In this task, Spaun is presented with two groups of three related items and must learn the relation between items in the groups. Spaun then uses its inferred relation to complete the pattern of a third set of items. Similarity plots for the DLPFC show conceptual decodings of neural activities. The model learns the relation between subsequent strings of numbers by comparing patterns in DLPFC1 and DLPFC2 (see supplementary section S1.3). Human participants average 89% correct (chance is 13%) on the matrices that include only an induction rule (5 of 36 matrices) (*16*). Spaun performs similarly, achieving a match-adjusted success rate of 88% (see supplementary section S2.3).

To demonstrate that Spaun captures general psychological features of behavior, it is critical to be able to simulate populations of participants. Every time a specific instance of Spaun is generated, the parameters of the neurons are picked from random distributions (supplementary section S1.4). Consequently, generating many instances allows for comparison with population-wide behavioral data. Figure 4 compares the recall accuracy of the model as a function of list length and position in a serial recall task to human population data. As with human data (*17*), Spaun produces distinct recency (items at the end are recalled with greater accuracy) and primacy

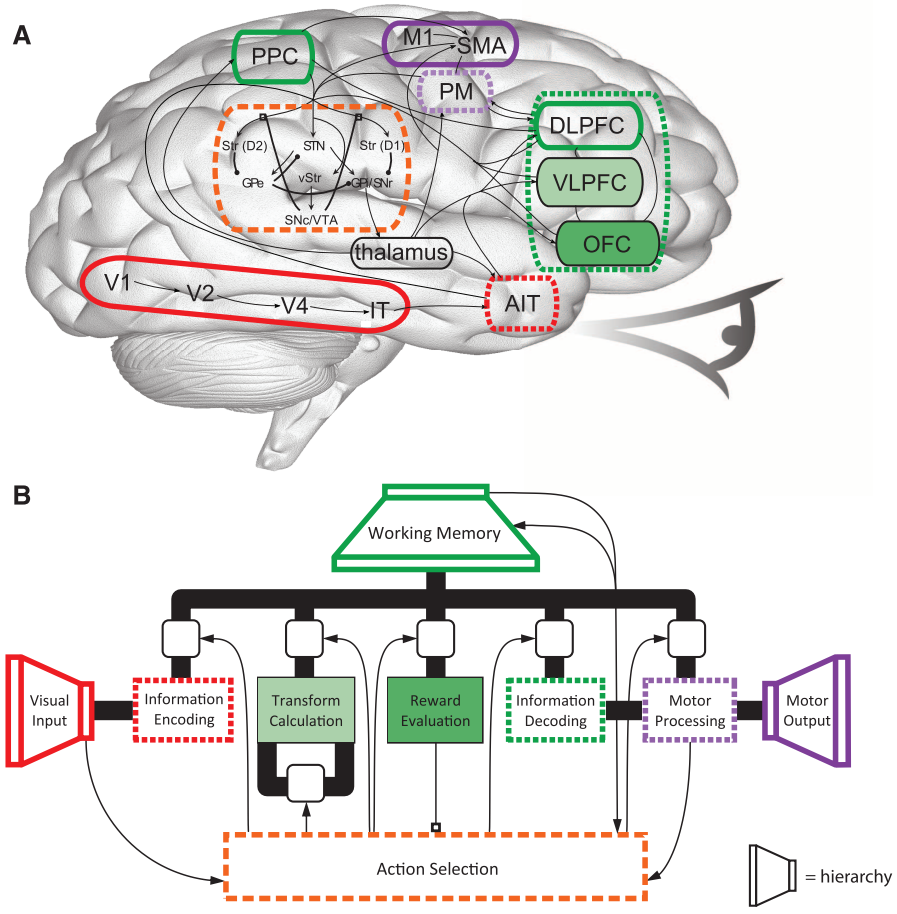


Fig. 1. Anatomical and functional architecture of Spaun. (**A**) The anatomical architecture of Spaun shows the major brain structures included in the model and their connectivity. Lines terminating in circles indicate GABAergic connections. Lines terminating in open squares indicate modulatory dopaminergic connections. Box styles and colors indicate the relationship with the functional architecture in (B). PPC, posterior parietal cortex; M1, primary motor cortex; SMA, supplementary motor area; PM, premotor cortex; VLPFC, ventrolateral prefrontal cortex; OFC, orbitofrontal cortex; AIT, anterior inferior temporal cortex; Str, striatum; vStr, ventral striatum; STN, subthalamic nucleus; GPe, globus pallidus externus; GPi, globus pallidus internus; SNr, substantia nigra pars reticulata; SNc, substantia nigra pars compacta; VTA, ventral tegmental area; V2, secondary visual cortex; V4, extrastriate visual cortex. (**B**) The functional architecture of Spaun. Thick black lines indicate communication between elements of the cortex; thin lines indicate communication between the action-selection mechanism (basal ganglia) and the cortex. Boxes with rounded edges indicate that the action-selection mechanism can use activity changes to manipulate the flow of information into a subsystem. The open-square end of the line connecting reward evaluation and action selection denotes that this connection modulates connection weights. See table S1 for more detailed definitions of abbreviations, a summary of the function to anatomy mapping, and references supporting Spaun's anatomical and functional assumptions.

(items at the beginning are recalled with greater accuracy) effects. A good match to human data from a rapid serial-memory task using digits and short presentation times (*18*) is also evident, with 17 of 22 human mean values within the 95% confidence interval of 40 instances of the model. Additional population comparisons are presented in fig. S8.

To this point, we have only described performance on three of the eight tasks that Spaun performs. The tasks not yet discussed are: (i) image recognition, for which the model achieves 94% accuracy on untrained data from the MNIST handwriting database [human accuracy is ~98% (*19*)]; (ii) RL, for which the model is able to learn reward-dependent actions in a variable environment using known neural mechanisms (fig. S5); (iii) counting, for which the model reproduces human reaction times and scaling of variability (fig. S8A); (iv) question answering, for which the model generates a novel behavioral prediction (fig. S8B); and (v) rapid variable creation, for which the model instantiates the first neural architecture able to solve this challenging task (fig. S11).

However, the central purpose of this work is not to explain any one of these tasks, but to propose a unified set of neural mechanisms able to perform them all. In a sense, the complex task solved by Spaun is one of coordination. That is, the rapid flexibility of biological systems is its target of explanation. The specific dynamics of Spaun's responses to this wide variety of tasks is governed by four parameters, each of which is set empirically (the time constants of the neurotransmitters; see supplementary section S2.4). Thus, without fitting, the model is consistent with dynamics from single cells and behavior (see figs. S8 and S11 and supplementary section S2.4), and is able to switch between a wide variety tasks quickly and robustly (fig. S10).

Although Spaun's main contribution lies in its breadth, it also embodies new hypotheses regarding how specific tasks are solved. For instance, the proposed method of solving the rapid variable-creation task is distinct to Spaun [this task has been identified as one that no contemporary neural architecture could perform as quickly as humans (*20*)], as is the account of serial WM. Such hypotheses have resulted in new testable predictions (figs. S8 and S9). Still, Spaun's uniqueness lies in its being a platform for exploring the robust flexibility of biological cognition. Consider the example of learning: Learning in Spaun takes on many forms. Although learning takes place in the RPM, rapid variable-creation, and RL, connection-weight changes only occur in the RL task (supplementary section S2.4). In most neural models, this kind of learning is often used as the main method of model construction, and it is possible to learn all of the elements of the Spaun model in this traditional sense (supplementary section S2.4). However, constructing models in this manner does not address a central, difficult challenge of learning in biological brains. That challenge consists of explaining how robust learning can occur in a continuously operating, complex, and multifunctional brain.

Spaun minimally demonstrates this kind of learning in the RL task, as connection-weight

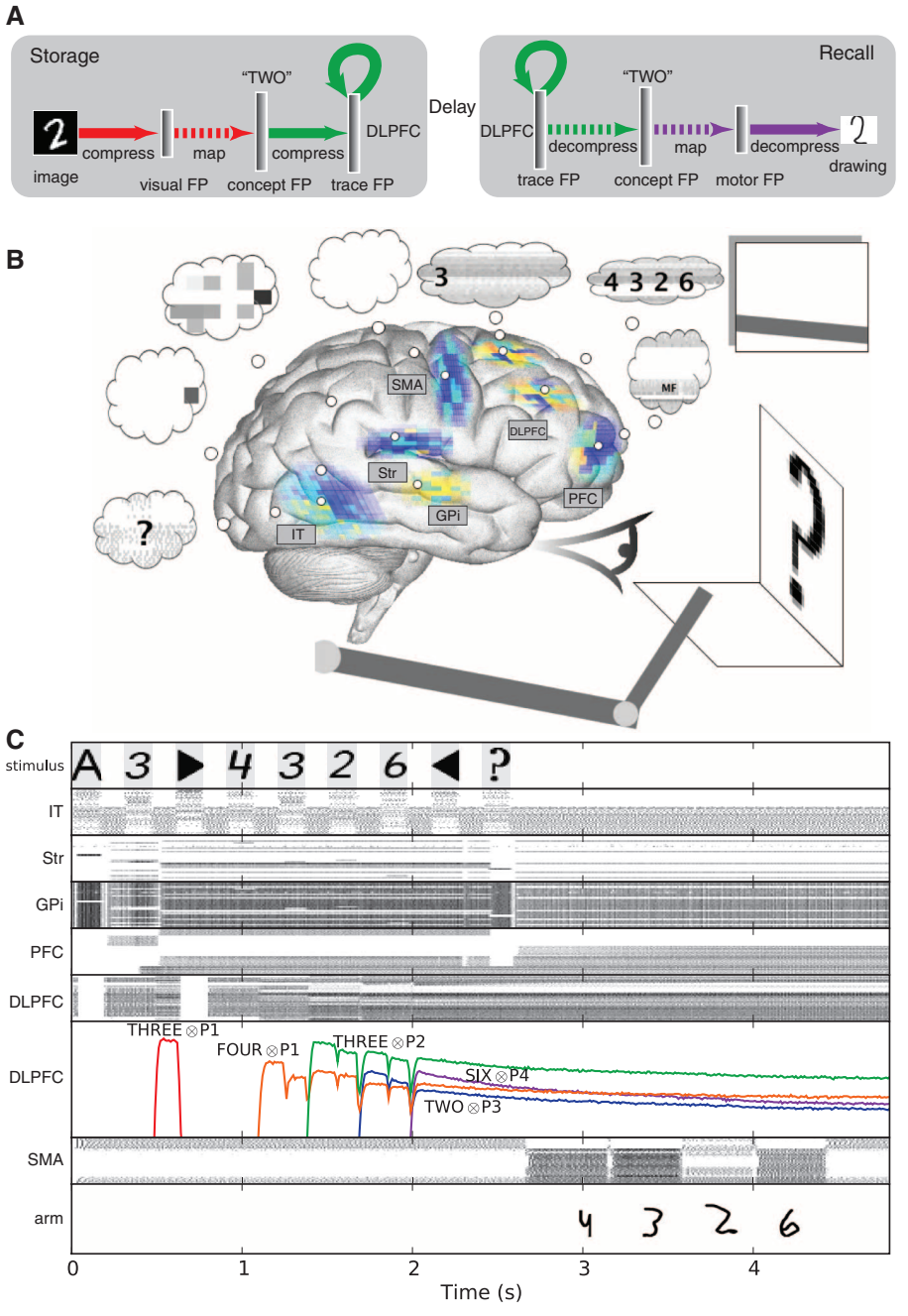


Fig. 2. The serial WM task. (**A**) Information flow through Spaun during the WM task. Line style and color indicate the element of the functional architecture in Fig. 1B responsible for that function. FP, firing pattern. (**B**) A screen capture from the simulation movie of this task (supplementary section S2.1), taken at the 2.5-s mark of the time course plot in (C). The input image is on the right, the output is drawn on the surface below the arm. Spatially organized (neurons with similar tuning are near one another), low-pass–filtered neuron activity is approximately mapped to relevant cortical areas and shown in color (red is high activity, blue is low). Thought bubbles show spike trains, and the results of decoding those spikes are in the overlaid text. For Str, the thought bubble shows decoded utilities of possible actions, and in GPi the selected action is darkest. (**C**) Time course of a single run of the serial WM task. The stimulus row shows input images. The arm row shows digits drawn by Spaun. Other rows are labeled by their anatomical area. Similarity plots (solid colored lines) show the dot product (i.e., similarity) between the decoded representation from the spike raster plot and concepts in Spaun's vocabulary. These plots provide a conceptual decoding of the spiking activity, but this decoding is not used by the model (supplementary section S1.1). Raster plots in this figure are generated by randomly selecting 2000 neurons from the relevant population and discarding any neurons with a variance of less than 10% over the run. ⊗ denotes the convolution compression operator.

changes do not adversely affect the performance of the model on other tasks. Smaller-scale models cannot provide even this minimal demonstration, because they lack the variety of tasks necessary to demonstrate robustness. As such, Spaun provides a distinct opportunity to test learning algorithms in a challenging but biologically plausible setting. More generally, Spaun provides an opportunity to test any neural theory that may be affected by being embedded in a complex, dynamical context, reminiscent of a real neural system.

However, Spaun has little to say about how that complex, dynamical system develops from birth. Furthermore, Spaun has many other limitations that distinguish it from developed brains. For one, Spaun is not as adaptive as a real brain, as the model is unable to learn completely new tasks. In addition, both attention and eye position of the model is fixed, making Spaun unable to control its own input. Also, its perceptual and conceptual representations are largely limited to the space of digits from 0 to 9. Anatomically, many areas of the brain are missing from the model. Those that are included have too few neurons and perform only a subset of functions found in their respective areas. Physiologically, the variability of spiking in the model is not always reflective of the variability observed in real brains (table S3). However, we believe that, as available computational power increases, many of these limitations can be overcome via the same methods as those used to construct Spaun (supplementary section S2.4).

Even in its current form, Spaun offers a distinctly functional view and set of hypotheses regarding the neural mechanisms and organization that may underlie basic cognitive functions. Consequently, Spaun opens new avenues for testing ideas about biological cognition under biologically plausible, more complex, and more functional settings than previously available.

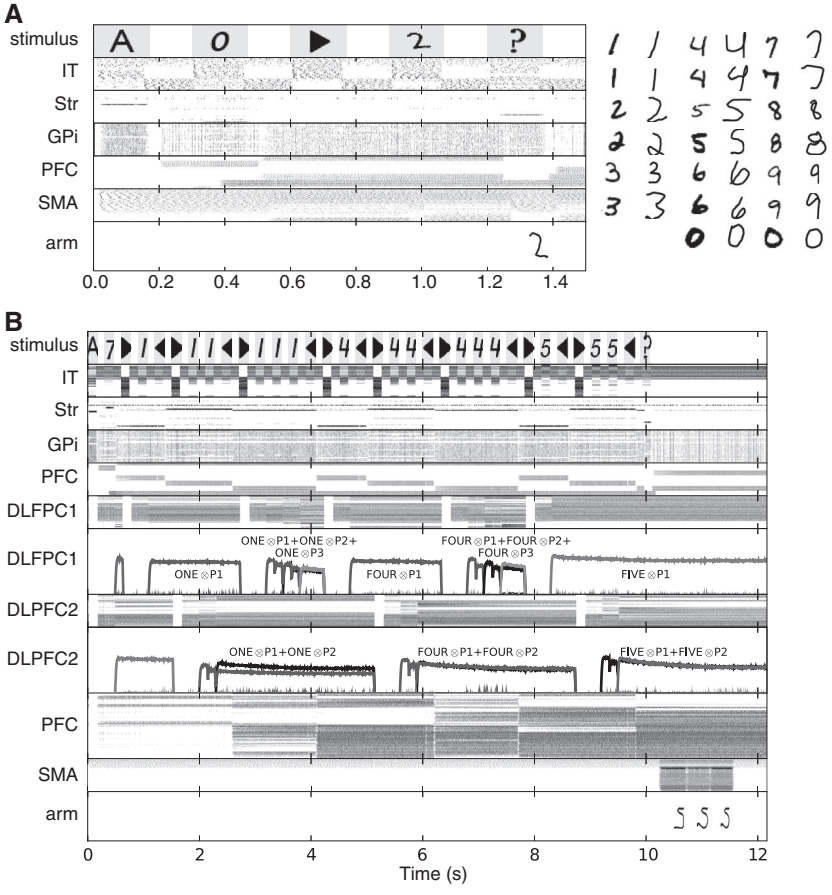


Fig. 3. Time-course plots for two Spaun tasks. (**A**) Results of the copy-drawing task. The input/output pairs for 20 additional runs are shown to the right. (**B**) Results of an example run of the RPM task, plotted using the same method as described in Fig. 2C. See text for details.

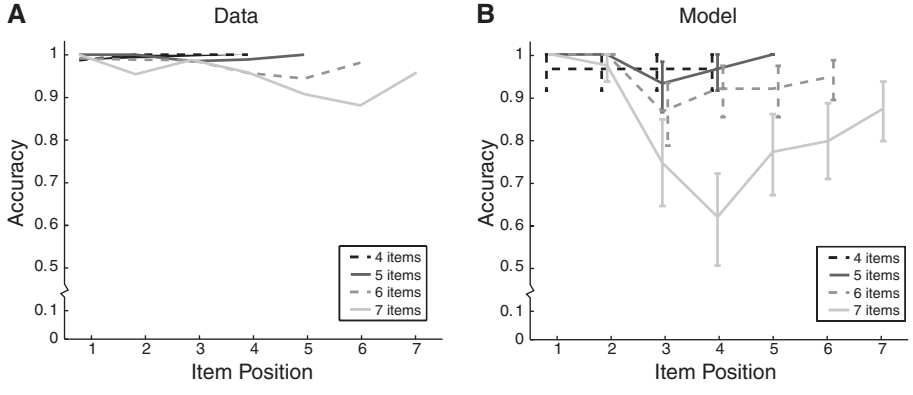


Fig. 4. Population-level behavioral data for the WM task. Accuracy is shown as a function of position and list length for the serial WM task. Error bars are 95% confidence intervals over 40 runs per list length. (**A**) Human data taken from (*18*) (only means were reported). (**B**) Model data showing similar primacy and recency effects.

References and Notes

1. H. de Garis, C. Shuo, B. Goertzel, L. Ruiting, *Neurocomputing* **74**, 3 (2010).
2. H. Markram, *Nat. Rev. Neurosci.* **7**, 153 (2006).
3. R. Ananthanarayanan, D. S. Modha, in *Proceedings of the 2007 ACM/IEEE Conference on Supercomputing-SC '07* (Association for Computing Machinery Press, New York, 2007), p. 1.
4. E. M. Izhikevich, G. M. Edelman, *Proc. Natl. Acad. Sci. U.S.A.* **105**, 3593 (2008).
5. M. Ranzato, Y. Boureau, Y. LeCun, *Adv. Neural Inf. Process. Syst.* **20**, 1 (2007).
6. G. E. Hinton, R. R. Salakhutdinov, *Science* **313**, 504 (2006).
7. T. Orlov, V. Yakovlev, D. Amit, S. Hochstein, E. Zohary, *Cereb. Cortex* **12**, 306 (2002).
8. B. B. Murdock, *Psychol. Rev.* **100**, 183 (1993).
9. W. Schultz, *Nat. Rev. Neurosci.* **1**, 199 (2000).
10. E. Vasilaki, N. Frémaux, R. Urbanczik, W. Senn, W. Gerstner, *PLOS Comput. Biol.* **5**, e1000586 (2009).
11. J. Raven, J. Court, *Manual for Raven's Progressive Matrices and Vocabulary Scales* (Harcourt Assessment, San Antonio, TX, 2004).
12. T. Pasternak, J. Bisley, D. Calkins, in *Handbook of Psychology, Biological Psychology*, M. Gallagher, R. J. Nelson, Eds. (Wiley, Hoboken, NJ, 2003), vol. 3, pp. 139–185.
13. E. Todorov, *The Cognitive Neurosciences*, M. S. Gazzaniga, Ed. (MIT Press, Cambridge, MA, 2009).
14. T. Stewart, T. Bekolay, C. Eliasmith, *Front. Decis. Neurosci.* **6**, article no. 00002 (2012); 10.3389/fnins.2012.00002.
15. D. MacNeil, C. Eliasmith, *PLoS ONE* **6**, e22885 (2011).
16. A. R. Forbes, *Br. J. Educ. Psychol.* **34**, 223 (1964).
17. J. C. Jahnke, *J. Exp. Psychol.* **76**, 618 (1968).
18. B. A. Dosher, *Int. J. Psychol.* **34**, 276 (1999).
19. I. Chaaban, M. R. Scheessele, "Human performance on the USPS database" (Technical Report, Indiana Univ., South Bend, IN, 2007).
20. R. F. Hadley, *Neural Comput.* **21**, 510 (2009).

Acknowledgments: The development of Spaun was supported by the Natural Sciences and Engineering Research Council of Canada, the Canada Research Chairs program, the Canadian Foundation for Innovation, and the Ontario Innovation Trust. We thank M. van der Meer, B. Tripp, M. Laubach, and three anonymous reviewers for insightful comments on previous drafts. All models, scripts, and videos are deposited online at http://nengo.ca/ and http://models.nengo.ca/.

Supplementary Materials

www.sciencemag.org/cgi/content/full/338/6111/1202/DC1
Materials and Methods
Supplementary Text
Figs. S1 to S12
Tables S1 to S3
References (*21*–*74*)
Movies S1 to S8 (at http://nengo.ca/build-a-brain/spaunvideos)

28 May 2012; accepted 15 October 2012
10.1126/science.1225266